



**HAL**  
open science

## On the Use of the Power-Law Model for Interpreting Constant-Phase-Element Parameters

Mark E. Orazem, Bernard Tribollet, Vincent Vivier, Douglas P. Riemer, Erick  
White, Annette Bunge

► **To cite this version:**

Mark E. Orazem, Bernard Tribollet, Vincent Vivier, Douglas P. Riemer, Erick White, et al.. On the Use of the Power-Law Model for Interpreting Constant-Phase-Element Parameters. Journal of the Brazilian Chemical Society, 2014, 25 (3), pp.532-539. 10.5935/0103-5053.20140021 . hal-01017759

**HAL Id: hal-01017759**

**<https://hal.sorbonne-universite.fr/hal-01017759>**

Submitted on 20 Nov 2015

**HAL** is a multi-disciplinary open access archive for the deposit and dissemination of scientific research documents, whether they are published or not. The documents may come from teaching and research institutions in France or abroad, or from public or private research centers.

L'archive ouverte pluridisciplinaire **HAL**, est destinée au dépôt et à la diffusion de documents scientifiques de niveau recherche, publiés ou non, émanant des établissements d'enseignement et de recherche français ou étrangers, des laboratoires publics ou privés.



Distributed under a Creative Commons Attribution - NonCommercial 4.0 International License

## On the Use of the Power-Law Model for Interpreting Constant-Phase-Element Parameters

Mark E. Orazem,<sup>\*a</sup> Bernard Tribollet,<sup>b</sup> Vincent Vivier,<sup>b</sup> Douglas P. Riemer,<sup>c</sup>  
Erick White<sup>d</sup> and Annette Bunge<sup>d</sup>

<sup>a</sup>Department of Chemical Engineering, University of Florida, Gainesville, FL, 32611, USA

<sup>b</sup>LISE, UPR 15 du CNRS, Université P. et M. Curie, CP 133, 4 Place Jussieu, 75252 Paris, France

<sup>c</sup>Hutchinson Technology, Inc., 40 West Highland Park Dr. NE, Hutchinson, MN 55350, USA

<sup>d</sup>Department of Chemical and Biological Engineering, Colorado School of Mines,  
Golden, CO 80401, USA

Elementos de fase constante (CPE) são frequentemente usados para modelar dados de impedância oriundos de uma gama variada de sistemas experimentais. O modelo de lei de potências comprovou ser uma ferramenta poderosa na interpretação de parâmetros de CPE resultantes de uma distribuição axial ou normal das constantes de tempo. Este trabalho trata das dificuldades na aplicação deste modelo quando um de seus parâmetros possui valor incerto. São apresentados métodos que delimitam o valor do parâmetro, de calibração e de análise comparativa, na qual o parâmetro desconhecido pode ser eliminado. Os métodos são demonstrados por dados sobre óxidos em aços e sobre pele humana, retirados da literatura.

Constant-phase elements (CPE) are often used to fit impedance data arising from a broad range of experimental systems. The power-law model has proven to be a powerful tool for interpretation of CPE parameters resulting from an axial or normal distribution of time constants. This paper addresses difficulties in applying this model associated with uncertain values for one of the model parameters. Methods are presented for bounding the value of the parameter, for calibration, and for comparative analysis in which the unknown parameter may be eliminated. The methods are illustrated by data taken from the literature for oxides on steels and for human skin.

**Keywords:** electrochemistry, electro-analytical, voltammetry/amperometry/spectrophotometry/potentiometry analysis

### Introduction

In 2010, Hirschorn *et al.*<sup>1,2</sup> identified a relationship between constant-phase element (CPE) parameters and physical properties of films by regressing a measurement model<sup>3,4</sup> to synthetic CPE data. Following the procedure described by Agarwal *et al.*,<sup>3,4</sup> sequential Voigt elements were added to the model until the addition of an element did not improve the fit and one or more model parameters included zero within their 95.4 percent 2σ confidence interval.

Their concept was to identify the distribution of resistivity that, under the assumption that the dielectric constant is independent of position, would result in CPE behavior. The development is presented in detail in reference 1. The authors proposed a distribution of resistivity to be

$$\frac{\rho}{\rho_{\delta}} = \left( \frac{\rho_{\delta}}{\rho_0} + \left( 1 - \frac{\rho_{\delta}}{\rho_0} \right) \xi^{\gamma} \right)^{-1} \quad (1)$$

where  $\rho_0$  and  $\rho_{\delta}$  are the boundary values of resistivity at the interfaces. A graphical representation of the resistivity distribution associated with equation 1 is presented in Figure 1, where  $\rho_{\delta}$  is the resistivity at  $y = \delta$  or  $\xi = 1$ , and  $\rho_0$  is the resistivity at  $y = 0$  or  $\xi = 0$ . The value of  $\rho_0$  was

\*e-mail: meo@che.ufl.edu

chosen for this representation to be  $5 \times 10^4 \rho_\delta$ , but often  $\rho_0$  is too large to be seen in the impedance response.

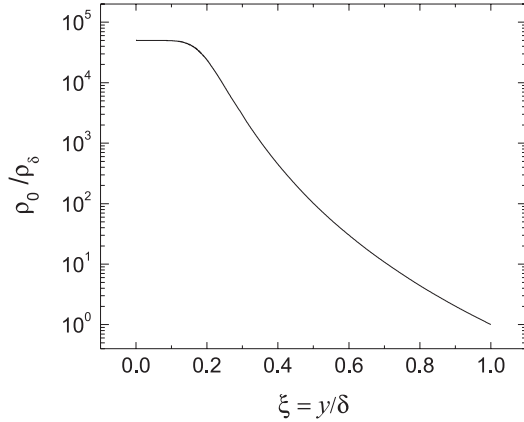


**Figure 1.** Graphical representation of the resistivity distribution associated with equation 1 where  $\rho_\delta$  is the resistivity at  $y = \delta$  or  $\xi = 1$ , and  $\rho_0$  is the resistivity at  $y = 0$  or  $\xi = 0$ . The value of  $\rho_0$  was chosen for this representation to be  $5 \times 10^4 \rho_\delta$ , but often  $\rho_0$  is too large to be seen in the impedance response.

Under the conditions that  $\rho_0 > \rho_\delta$  and  $f < (2\pi\rho_\delta\epsilon\epsilon_0)^{-1}$ , the impedance of the film was given as

$$Z_f(f) = g \frac{\delta\rho_\delta^{1/\gamma}}{(\rho_0^{-1} + j2\pi f\epsilon\epsilon_0)^{(\gamma-1)/\gamma}} \quad (2)$$

where  $g$  is a function of  $\gamma$ . Equation 2 was shown to be in the form of a CPE, i.e.,

$$Z_{\text{CPE}} = \frac{1}{(j2\pi f)^\alpha Q} \quad (3)$$

for  $f < (2\pi\rho_0\epsilon\epsilon_0)^{-1}$ . Examination of equation 3 and the high-frequency limit of equation 2 yielded  $1/\gamma = 1 - \alpha$  where  $\gamma \geq 2$  for  $0.5 \leq \alpha \leq 1$ . Numerical integration was used to develop the interpolation formula

$$g = 1 + 2.88(1 - \alpha)^{2.375} \quad (4)$$

A relationship among the CPE parameters  $Q$  and  $\alpha$  and the dielectric constant  $\epsilon$ , resistivity  $\rho_\delta$ , and film thickness  $\delta$  was found to be

$$Q = \frac{(\epsilon\epsilon_0)^\alpha}{g\delta\rho_\delta^{1-\alpha}} \quad (5)$$

where resistivity  $\rho_\delta$  is the lower bound for the resistivity given in equation 1 and  $\epsilon_0$  is the permittivity of vacuum with a value of  $\epsilon_0 = 8.8542 \times 10^{-14}$  F cm<sup>-1</sup>.

Orazem *et al.*<sup>5</sup> recently provided a summary of methods used to extract system properties from CPE parameters.

Following the concepts described by Jorcin *et al.*,<sup>6</sup> CPE behaviors were described as resulting from surface or normal (axial) distributions of time constants. If the CPE results from a dielectric response of the material, i.e., a normal distribution of time constants, it allows determination of an effective capacitance expressed in terms of dielectric constant  $\epsilon$  and film thickness  $\delta$  as

$$C_{\text{eff}} = \frac{\epsilon\epsilon_0}{\delta} \quad (6)$$

If the CPE response is instead associated with a surface distribution of time constants, a double-layer capacitance may be identified, and the associated value may be used to assess the electrochemically active area.

Equations 5 and 6 yield an expression for the effective capacitance as

$$C_{\text{eff,PL}} = gQ(\rho_\delta\epsilon\epsilon_0)^{1-\alpha} \quad (7)$$

In addition to the CPE parameters  $Q$  and  $\alpha$ ,  $C_{\text{eff,PL}}$  depends on the dielectric constant  $\epsilon$  and the smaller value of the resistivity  $\rho_\delta$ . A special feature of equation 7 is that it depends only on the high-frequency data without need for the resistance obtained at low frequency.

The assumption of a uniform dielectric constant is not critical to the development summarized above. Musiani *et al.*<sup>7</sup> have shown that equation 5 applies, even when the assumption of a uniform dielectric constant is relaxed by allowing variation of  $\epsilon$  in the region of low resistivity. The power-law model has been demonstrated to provide a suitable approach for interpreting the CPE behavior associated with the dielectric response of a film.<sup>2,5</sup> Indeed, the model has been adapted successfully to explore the role of water uptake in coatings.<sup>8</sup> While the power-law model provides a better interpretation of CPE parameters than does the formula derived from the characteristic frequency of the impedance, i.e.,

$$C_{\text{eff,norm}} = Q^{1/\alpha} R_{\parallel}^{(1-\alpha)/\alpha} \quad (8)$$

which is equivalent to equation 3 in the work of Hsu and Mansfeld,<sup>9</sup> it requires a parameter  $\rho_\delta$  that has well-defined physical meaning but is generally unknown.

In previous work,<sup>2</sup> the experimental frequency range was coupled with physical insight to establish a range of values for  $\rho_\delta$ . The authors also used independent measurements of film thickness to allow determination of a value for  $\rho_\delta$ , but this approach may be criticized if the uncertainty in the film-thickness measurement is very large. The object of this work is to explore the propagation of errors from the film-thickness measurement to determination of  $\rho_\delta$  and,

ultimately, to the estimation of film thickness for other systems. An alternative approach is also explored in which determination of  $\rho_8$  may be avoided. This work is intended to demonstrate how the power-law model may be applied to interpretation of CPE behavior.

## Experimental

The experimental results discussed in the present work come from the literature.

### Impedance of free-machining steel

Steel samples were masked using a vinyl tape, 0.132 mm thick, (3M 471) in which a precision 3 mm hole was cut. The coupon with applied mask was then sandwiched into a cell where 1 mL of electrolyte was used to fill the cell. The cell was attached to a PAR 2273 Potentiostat/FRA and impedance measurements were conducted at the measured open-circuit potential using a 10 mV perturbation.

Impedance data were collected in an electrolyte consisting of 22 g L<sup>-1</sup> boric acid with NaOH added, about 6 g L<sup>-1</sup>, to bring the pH to 7.2. The samples included steel in as-received condition and after a proprietary treatment to increase the chromium content of the oxide film. Additional information is provided in reference 5.

### Impedance of human skin

The impedance data reported in the present work came from a larger study intended to correlate changes in the flux of *p*-chloronitrobenzene (PCNB) and 4-cyanophenol in response to physical and chemical damage.<sup>10-12</sup> Split-thickness human cadaver skin (300-400  $\mu\text{m}$  thick) from the back or abdomen was purchased from the National Disease Research Interchange (NDRI, Philadelphia, PA). The skin was collected within 24 h post mortem, frozen immediately, and stored at temperatures less than  $-60^\circ\text{C}$  until used. The protocol described by White *et al.*<sup>10</sup> was used to ensure that the skin resistance was greater than 20 k $\Omega$  cm<sup>2</sup>, a value considered to indicate that samples have sufficient integrity for meaningful measurements of in-vitro chemical permeability.

The impedance was measured in a four-electrode configuration, in which two Ag/AgCl (In Vivo Metric, Healdsburg, CA) reference electrodes were used to sense the potential drop across the skin, and two Ag/AgCl working electrodes were used to drive the current. Ag/AgCl electrodes are commonly used for biological systems because the electrolytes typically contain chloride ions and the associated electrochemical reactions do not

change the electrolyte pH. The skin was exposed on both sides for roughly eight hours to a phosphate buffered saline solution (PBS) (0.01 mol L<sup>-1</sup>, pH 7.4, Sigma P-3813) prepared in deionized water.

### Mechanical damage

The impedance measurements reported here were collected with a 10 mV potential perturbation after two permeation experiments (for 7 and 6 h, respectively) in which 4-cyanophenol-saturated PBS was placed in the donor chamber and PBS was placed in the receptor chamber. After the first 4-cyanophenol permeation experiment, the frame holding the skin was removed from the diffusion cell, the skin was pierced by a 26 gauge needle (with a 464  $\mu\text{m}$  outside diameter), the cell was reassembled, and the donor and receptor chambers refilled with fresh 4-cyanophenol-saturated PBS and PBS, respectively, for the second permeation experiment. Typical results show that the characteristic frequency before the puncture was substantially smaller than the characteristic frequency after the puncture.

Because the diameter of the needle used to puncture the skin was small compared to the total skin area, the pinhole was expected to have little effect on the impedance properties of the remaining skin. Control experiments were used to show that the electrical properties of skin were unaffected by other skin handling steps. Therefore, the skin resistance and the dielectric constant for the skin were assumed to be the same before and after the skin was pierced by the needle. Additional experimental detail can be found in reference 11.

### Chemical damage

The dimethyl sulfoxide (DMSO) experiments consisted of simultaneous measurements of impedance and PCNB flux through skin before and after 1 h treatments with 100% DMSO or with PBS, which acted as the control. The entire experiment was repeated three times. Before the measurements, skin was allowed to equilibrate by immersion in PBS for an eight to twelve hour period.

After equilibration, both chambers were emptied and the receptor and donor chambers were rinsed and filled with 13 mL of PBS and PCNB-saturated PBS, respectively. To ensure saturation of the donor solution throughout the experiment, excess crystals of PCNB were added to the donor chamber solution. After treatment for 1 h, the frame holding each skin sample, including the PBS controls, was removed from the diffusion cell assembly and soaked in approximately 1 L of fresh deionized water three times for

0.25 h and then for 1 h in about 1 L of PBS. The diffusion cells were rinsed thoroughly and then reassembled and filled with PBS solution for another 8-h equilibration period with hourly impedance scans. Impedance results reported for before and after DMSO treatment were derived from the last spectrum collected during the equilibration periods. Additional experimental detail can be found in reference 12.

## Results and Discussion

Values for  $Q$  and  $\alpha$  are obtained from impedance measurements. If the dielectric constant is known, equation 5 may be used to extract  $\delta\rho_{\delta}^{(1-\alpha)}$ . To obtain the film thickness  $\delta$ , a value for  $\rho_{\delta}$  is required. If  $\delta$  is known, equation 5 yields a value for  $\epsilon^{\alpha}/\rho_{\delta}^{(1-\alpha)}$ . To obtain the dielectric constant  $\epsilon$ , a value for  $\rho_{\delta}$  is required. The principal difficulty in the application of the power-law model is that values for the parameter  $\rho_{\delta}$  are unknown. Several methods are proposed to address this difficulty. The frequency range over which CPE behavior is observed may be used to establish an upper bound for the value of  $\rho_{\delta}$ . If the film thickness  $\delta$  and dielectric constant  $\epsilon$  are known for a material similar to that under investigation, the value of  $\rho_{\delta}$  may be obtained through calibration. If calibration is not possible, the power-law model may be used to guide comparative studies.

### Establishing bounds

Hirschorn *et al.*<sup>1</sup> demonstrated the method by which bounds on the value of  $\rho_{\delta}$  may be established through high-frequency limit of the impedance response. The impedance response of the power law model exhibits capacitive behavior above a characteristic frequency

$$f_{\delta} = \frac{1}{2\pi\rho_{\delta}\epsilon\epsilon_0} \quad (9)$$

Under conditions that the value of  $\rho_{\delta}$  is unknown for data showing high-frequency CPE behavior, an upper bound on its value can be defined because the characteristic frequency  $f_{\delta}$  must be larger than the largest measured frequency  $f_{\max}$ . Thus, a maximum value of  $\rho_{\delta}$  can be obtained

$$\rho_{\delta,\max} = \frac{1}{2\pi\epsilon\epsilon_0 f_{\max}} \quad (10)$$

Hirschorn *et al.*<sup>2</sup> applied this approach for data that were presented by Frateur *et al.*<sup>13</sup> for the impedance response of a Fe17Cr disk (polarized in the passive domain for 1 h at  $-0.1$  V measured with respect to a mercury/mercurous sulfate electrode in saturated  $K_2SO_4$ )

in deaerated pH 4,  $0.05 \text{ mol L}^{-1} Na_2SO_4$  electrolyte. A value of 12 was assumed for  $\epsilon$ , which corresponds to the dielectric constant for  $Fe_2O_3$  and  $Cr_2O_3$ . For this experiment, with a maximum measurement frequency of 100 kHz,  $\rho_{\delta,\max} = 1.5 \times 10^6 \Omega \text{ cm}$ . A lower bound for  $\rho_{\delta}$  may also be estimated on physical grounds. For an oxide, for example,  $\rho_{\delta}$  is not expected to be smaller than minimum resistivity value expected for semiconductors, i.e.,  $1 \times 10^{-3} \Omega \text{ cm}$ . Using equation 5, this conservative range of  $\rho_{\delta}$  yields an estimated layer thickness of  $\delta = 1.2$  to 12.6 nm, which encompasses the value of 3 nm obtained from X-ray photoelectron spectroscopy (XPS).<sup>13</sup> While it is satisfying that a physically reasonable range of film thickness can be identified by the methods discussed by Hirschorn *et al.*,<sup>2</sup> more precise values are desired.

For the impedance data associated with human skin in PBS, the thickness of the stratum corneum may be assumed to be around 15  $\mu\text{m}$ , but the dielectric constant is not known. In this case, equations 5 and 10 must be solved simultaneously. Using an iterative technique, the maximum measured frequency yielded  $\rho_{\delta} = 1.59 \times 10^5 \Omega \text{ cm}$ , corresponding to a dielectric constant of 122. The lowest value for  $\rho_{\delta}$  was selected on the grounds that the resistivity of the skin should approach that of the electrolyte in which it is immersed; i.e.,  $\rho_{\delta} = 55 \Omega \text{ cm}$ , corresponding to a dielectric constant of 22. In this case, the range of values obtained is too large to be meaningful, and, again, a more precise approach is desired.

### Calibration

From XPS analysis, Frateur *et al.*<sup>13</sup> showed that the passive film developed on Fe17Cr consisted of an inner layer of  $Fe_2O_3$  and  $Cr_2O_3$  covered by an outer layer of  $Cr(OH)_3$  and that the thickness was about 3 nm. Graphical analysis of the impedance yielded  $\alpha = 0.89$  and  $Q = 3.7 \times 10^{-5} \text{ F cm}^{-2} \text{ s}^{-0.11}$ . Equation 5 was used to obtain  $\rho_{\delta} = 450 \Omega \text{ cm}$ . Under the assumption that other oxides on steel will have similar values for  $\rho_{\delta}$ , this value of  $\rho_{\delta}$  was used in subsequent analysis of the impedance response free-machining 18/8 stainless steel (18 Cr-8 Ni), also known as 303 stainless steel, and martensitic stainless steel.<sup>5</sup> The power-law model yielded good agreement to independent values of film thickness measured by use of *ex-situ* XPS.

Assessment of film thickness by XPS, however, is imprecise, and uncertainties in the measurement used for calibration should propagate to the value of  $\rho_{\delta}$ . Monte Carlo simulations were performed to illustrate the manner in which uncertainty in the measurement of the film thickness causes uncertainty in the resulting  $\rho_{\delta}$ . Under the assumptions that the standard deviation on the assessment

of film thickness by XPS is 10% of the measured value and that the errors are normally distributed, the assessment of film thickness can be expressed as shown in Figure 2.

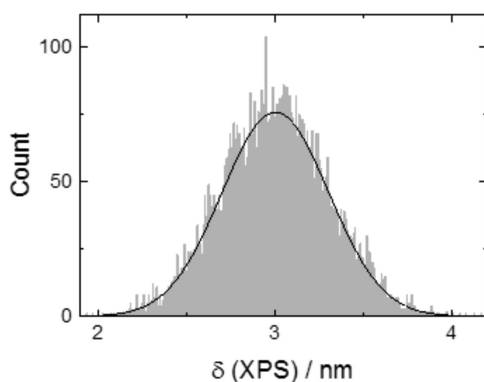


**Figure 2.** Histogram of the oxide film thickness measured by XPS and used to calibrate the power-law model. The standard deviation of the measurement was assigned a value of 10%, and the errors were assumed normally distributed.

Under the additional assumption that the dielectric constant of the oxide was  $\epsilon = 12$ , the resulting value of  $\rho_\delta$ , obtained from equation 5, was found to be log-normally distributed, as shown in Figure 3a. The corresponding distribution of the logarithm of  $\rho_\delta$  is shown in Figure 3b. The 10% uncertainty of the film thickness used to calibrate the power-law model results in an uncertainty of  $\rho_\delta$  that extends over two orders of magnitude. The large uncertainty in  $\rho_\delta$  shown in Figure 3 can be attributed to the observation that, in equation 5,  $\rho_\delta$  appears raised to the  $1-\alpha$  power. When  $\alpha$  is close to unity, equation 5 is relatively insensitive to  $\rho_\delta$ .

The calibration from the data of Frateur *et al.*<sup>13</sup> was used by Orazem *et al.*<sup>5</sup> to estimate the thickness of films on a free-machining 18/8 stainless steel (18 Cr-8 Ni). They regressed the data with the equation

$$Z = R_c + \frac{R_{||}}{1 + (j2\pi f)^\alpha R_{||} Q} \quad (11)$$

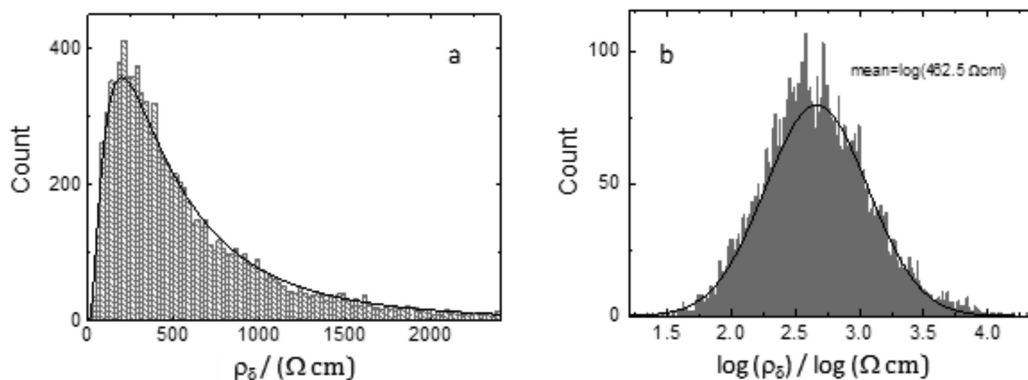


**Figure 3.** The distributed value of  $\rho_\delta$  obtained from the thickness values shown in Figure 1 through equation 5 under the assumption that  $\epsilon = 12$ : a) histogram of  $\rho_\delta$ ; and b) histogram of  $\log \rho_\delta$ .

where  $R_{||}$  is the parallel resistance. The results are presented in Table 1. The film thickness obtained by *ex-situ* XPS measurements are also reported. The dielectric constant was assumed to have a value  $\epsilon = 12$ . As shown in Figure 4, the uncertainty in  $\rho_\delta$  illustrated in Figure 3 is propagated to the estimate of film thickness, as reported in Table 1. The insensitivity of equation 5 to  $\rho_\delta$ , which resulted in a large uncertainty shown in Figure 3, also explains the small standard deviation revealed in Figure 4. The mean value of the film thickness obtained by the power-law model is in good agreement with the value obtained by *ex-situ* XPS, and the uncertainty in the estimated value is of the order of the uncertainty in the original XPS measurement.

**Table 1.** Regression results for free-machining 18/8 stainless steel in an electrolyte consisting of 22 g L<sup>-1</sup> boric acid with NaOH added to bring the pH to 7.2.<sup>5</sup>

|   | As received   | After proprietary treatment |
|---|---------------|-----------------------------|
| $R_c / (\Omega \text{ cm}^2)$                   | 15.3          | 13.3                        |
| $R_{  } / (\text{M}\Omega \text{ cm}^2)$        | 2.33          | 16.8                        |
| $\alpha$  | 0.91          | 0.91                        |
| $Q / (\mu\text{F s}^{(1-\alpha)} \text{ cm}^2)$ | 11            | 30.5                        |
| $\delta_{\text{XPS}} / \text{nm}$               | 6.3           | 2.5                         |
| $\delta_{\text{PL}} / \text{nm}$                | $5.9 \pm 0.5$ | $2.7 \pm 0.2$               |

While the emphasis in the present work was on the effect of uncertainty in the value of  $\rho_\delta$  on assessment of film thickness, a similar Monte Carlo analysis could be applied for estimation of dielectric constant when film thickness is known. A Monte Carlo analysis may also be used to address uncertainty in other parameters, for example, in both  $\rho_\delta$  and  $\epsilon$  for estimation of film thickness.

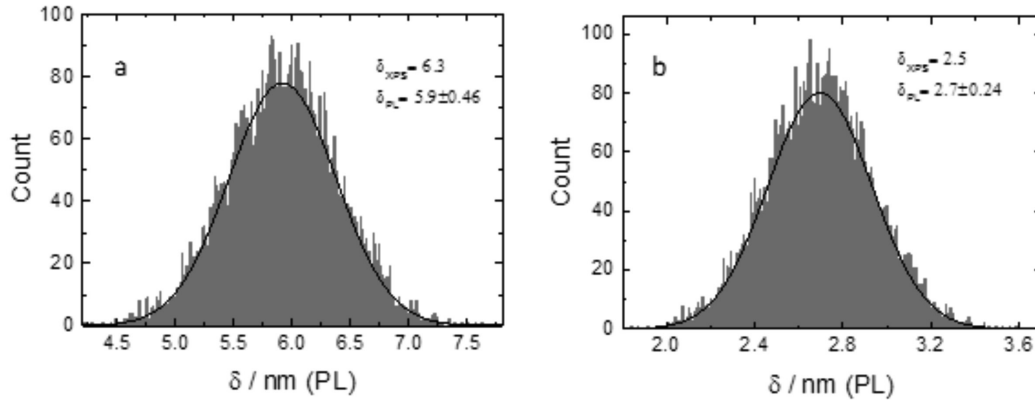


**Figure 4.** Histogram of film thickness estimated by use of equation 5 under the assumptions that  $\varepsilon = 12$  and that  $\rho_\delta$  is given as shown in Figure 2: a) steel in as-received condition; and b) steel after a proprietary treatment to increase the chromium content of the oxide film.

### Comparative analysis

When a reliable value for  $\rho_\delta$  is unavailable, useful information may still be obtained by taking ratios. For example, the ratio of film thickness may be obtained from equation 5 to be

$$\frac{\delta_1}{\delta_2} = \frac{(\varepsilon_1 \varepsilon_0)^{\alpha_1} g_2 Q_2 \rho_{\delta,2}^{(1-\alpha_2)}}{(\varepsilon_2 \varepsilon_0)^{\alpha_2} g_1 Q_1 \rho_{\delta,1}^{(1-\alpha_1)}} \quad (12)$$

If film properties  $\varepsilon$  and  $\rho_\delta$  may, respectively, be assumed equal for the two samples,

$$\frac{\delta_1}{\delta_2} = \frac{g_2 Q_2}{g_1 Q_1} (\varepsilon \varepsilon_0 \rho_\delta)^{\alpha_1 - \alpha_2} \quad (13)$$

If  $\alpha_1 = \alpha_2$ , then  $g_1 = g_2$ , and values for  $\varepsilon$  and  $\rho_\delta$  are not required. Thus,

$$\frac{\delta_1}{\delta_2} = \frac{Q_2}{Q_1} \quad (14)$$

From Table 1,  $\alpha_1 = \alpha_2$ . Under the assumptions that the surface treatment did not change the dielectric constant of the film and that the value of  $\rho_\delta$  is the same for the two films, equation 14. For the data presented in Table 1,  $Q_2/Q_1 = 28$ , which is in good agreement with the ratio of corresponding film thickness measured by XPS of  $6.3/2.5 = 2.5$ . This work shows that film thickness is inversely proportional to the value of  $Q$ .

A similar approach is available when the dielectric constant is the desired quantity. The ratio of values of dielectric constant can be expressed through equation 5 as

$$\frac{\varepsilon_1}{\varepsilon_2} = \frac{(Q_1 g_1 \delta_1)^{1/\alpha_1} \rho_{\delta,1}^{(1-\alpha_1)/\alpha_1}}{(Q_2 g_2 \delta_2)^{1/\alpha_2} \rho_{\delta,2}^{(1-\alpha_2)/\alpha_2}} \quad (15)$$

or, if the thickness and  $\rho_\delta$  are unchanged between measurements,

$$\frac{\varepsilon_1}{\varepsilon_2} = \frac{(Q_1 g_1)^{1/\alpha_1}}{(Q_2 g_2)^{1/\alpha_2}} (\delta \rho_\delta)^{(\alpha_2 - \alpha_1)/\alpha_1 \alpha_2} \quad (16)$$

Under the assumption that  $\alpha$ ,  $\delta$ , and  $\rho_\delta$  are unaffected by the different exposures,

$$\frac{\varepsilon_1}{\varepsilon_2} = \left( \frac{Q_1}{Q_2} \right)^{1/\alpha} \quad (17)$$

Equation 16 is very sensitive to differences in  $\alpha$  because  $Q$  and  $\alpha$  are highly correlated in the regression analysis. Thus, equation 17 should not be used when  $\alpha_1 \neq \alpha_2$ .

The implications of equation 15 can be explored through analysis of recently reported impedance data on human skin. Results are presented in Table 2 for regression of equation 11 to the impedance of skin before and after a) being pierced by a needle;<sup>11</sup> b) exposure to phosphate buffered saline solution (PBS) for a 1 h period;<sup>12</sup> and c) exposure to dimethyl sulfoxide (DMSO) for a 1 h period.<sup>12</sup> Values are the mean and one standard deviation of the parameter value for all exposed skin samples.

Under the assumption that  $\rho_\delta = 55 \Omega \text{ cm}$ , the dielectric constant for skin obtained by use of the power-law model (equation 7) ranged between 19 and 41, as reported in Table 2. These values are in good agreement with values between 29 and 44 reported in the literature that were obtained by reflection of 300 MHz electromagnetic radiation.<sup>14,15</sup> The value of dielectric constant obtained by use of equation 8, however, yielded physically unreasonable values ranging from 271 to 434. The standard deviations reported in Table 2 were obtained assuming a linear propagation of error with an assumed 10% uncertainty for the thickness of the stratum corneum.

**Table 2.** Results for regression of equation 11 to the impedance of human skin before and after a) being pierced by a needle (pinhole);<sup>11</sup> b) exposure to phosphate buffered saline solution (PBS) for a period of 1 hour;<sup>12</sup> and c) exposure to 100% dimethyl sulfoxide (DMSO) for a period of 1 hour.<sup>12</sup> Values are the mean and one standard deviation of the parameter value for all exposed skin samples. The standard deviations reported for the calculation of dielectric constant from equations 7 and 8 were obtained assuming a linear propagation of error with an assumed 10% uncertainty for the thickness of the stratum corneum

| Variable   | Pinhole <sup>11</sup> |                 | 1 hour PBS <sup>12</sup> |                 | 1 hour DMSO <sup>12</sup> |                 |
|--|-----------------------|-----------------|--------------------------|-----------------|---------------------------|-----------------|
|  | Before                | After           | Before                   | After           | Before                    | After           |
| $R_{  }$ / (k $\Omega$ cm <sup>2</sup> )                         | 118 $\pm$ 54          | 16.2 $\pm$ 5    | 147 $\pm$ 139            | 128 $\pm$ 120   | 153 $\pm$ 61              | 1.4 $\pm$ 0.15  |
| $\alpha$   | 0.816 $\pm$ 0.01      | 0.83 $\pm$ 0.01 | 0.87 $\pm$ 0.01          | 0.86 $\pm$ 0.01 | 0.87 $\pm$ 0.01           | 0.81 $\pm$ 0.01 |
| $Q$ / (nF s <sup>(1-<math>\alpha</math>)</sup> cm <sup>2</sup> ) | 74.4 $\pm$ 12.5       | 66.6 $\pm$ 10.5 | 43 $\pm$ 5               | 38 $\pm$ 7      | 38 $\pm$ 7                | 158 $\pm$ 28    |
| No. samples  | 7                     |                 | 3                        |                 | 3                         |                 |
| $\epsilon_1 / \epsilon_2$ , equation 16                          | 0.78                  |                 | 1.49                     |                 | 0.88                      |                 |
| $\epsilon$ , equation 8  | 433 $\pm$ 113         | 278 $\pm$ 68    | 342 $\pm$ 78             | 271 $\pm$ 68    | 298 $\pm$ 75              | 372 $\pm$ 102   |
| $\epsilon$ , equation 7  | 19 $\pm$ 7            | 24 $\pm$ 9      | 41 $\pm$ 13              | 27 $\pm$ 10     | 35 $\pm$ 13               | 40 $\pm$ 15     |

As the average value of  $\alpha$  was not constant between exposures, equation 17 could not be used to assess the ratio of dielectric constants before and after the treatments specified in Table 2. The ratios obtained by equation 16 are in good agreement with the values of dielectric constant calculated from equation 7.

## Conclusions

The power-law model given as equation 7 is a powerful tool for interpretation of CPE parameters for cases where the CPE response is due to an axial or normal distribution of time constants within a film. While equation 8 should in principle apply for a normal distribution of time constants, the formula provides incorrect results. Equation 8 has the advantage of being unambiguous, as every parameter required for the analysis can be obtained from regression of a CPE model to the data, but, as discussed above, it gives incorrect results for a CPE resulting from a normal distribution of time constants. For these cases, the power-law model provides correct results, but is ambiguous because the parameter  $\rho_\delta$  is unknown.

Three approaches were used in the present work to resolve issues caused by the unknown parameter  $\rho_\delta$ . The highest measured frequency that shows CPE behavior may be used to calculate an upper bound for the value of  $\rho_\delta$ , and physical insight into the experimental system may be used to estimate a lower limit. As film thickness is weakly dependent on  $\rho_\delta$ , identification of a range for  $\rho_\delta$  may be useful. A conservative estimate for the range of  $\rho_\delta$  associated with the data presented by Frateur *et al.*<sup>13</sup> yielded an estimated layer thickness of  $\delta = 1.2$  to 12.6 nm, which encompasses the value of 3 nm obtained from XPS. In other cases, the estimated range of  $\rho_\delta$  is too large. If an independent assessment of film

properties is possible, calibration may be used to obtain a value of  $\rho_\delta$ .

The third approach is to calculate ratios that allow cancellation of the unknown quantities. In the present work, the ratio of film thicknesses was found to be in good agreement with *ex-situ* XPS measurements, and a ratio of dielectric constants was ascertained for skin to be in good agreement with expected values.

## Acknowledgements

The authors gratefully acknowledge the support of the National Institute of Occupational Safety and Health Award No. R01 OH007493 (Bunge, White, and Orazem) and Hutchinson Technology, USA (Riemer).

## References

- Hirschorn, B.; Orazem, M. E.; Tribollet, B.; Vivier, V.; Frateur, I.; Musiani, M.; *J. Electrochem. Soc.* **2010**, *157*, C452.
- Hirschorn, B.; Orazem, M. E.; Tribollet, B.; Vivier, V.; Frateur, I.; Musiani, M.; *J. Electrochem. Soc.* **2010**, *157*, C458.
- Agarwal, P.; Orazem, M. E.; García-Rubio, L. H.; *J. Electrochem. Soc.* **1992**, *139*, 1917.
- Agarwal, P.; Crisalle, O. D.; Orazem, M. E.; García-Rubio, L. H.; *J. Electrochem. Soc.* **1995**, *142*, 4149.
- Orazem, M. E.; Tribollet, B.; Vivier, V.; Marcelin, S.; Pébère, N.; Bunge, A. L.; White, E. A.; Riemer, D. P.; Frateur, I.; Musiani, M.; *J. Electrochem. Soc.* **2013**, *160*, C215.
- Jorcín, J.-B.; Orazem, M. E.; Pébère, N.; Tribollet, B.; *Electrochim. Acta* **2006**, *51*, 1473.
- Musiani, M.; Orazem, M. E.; Pébère, N.; Tribollet, B.; Vivier, V.; *J. Electrochem. Soc.*, **2011**, *158*, C424.
- Amand, S.; Musiani, M.; Orazem, M. E.; Pébère, N.; Tribollet, B.; Vivier, V.; *Electrochim. Acta* **2013**, *87*, 693.



9. Hsu, C. H.; Mansfeld, F.; *Corrosion* **2001**, *57*, 747.
10. White, E. A.; Orazem, M. E.; Bunge, A. L.; *J. Electrochem. Soc.* **2012**, *159*, G161.
11. White, E. A.; Orazem, M. E.; Bunge, A. L.; *Pharm. Res.* **2013**, *30*, 2036.
12. White, E. A.; Orazem, M. E.; Bunge, A. L.; *Pharm. Res.* **2013**, *30*, 2607.
13. Frateur, I.; Lartundo-Rojas, L.; Méthivier, C.; Galtayries, A.; Marcus, P.; *Electrochim. Acta* **2006**, *51*, 1550.
14. Petäjä, L.; Nuutinen, J.; Uusaro, A.; Lahtinen, T.; Ruokonen, E.; *Physiol. Meas.* **2003**, *24*, 383.
15. Jensen, M. R.; Birkballe, S.; Nørregaard, S.; Karlsmark, T.; *Clin. Physiol. Funct. Imaging* **2012**, *32*, 317.

*Submitted: October 31, 2013*

*Published online: January 28, 2014*